The nitric oxide pathway modulates hemangioblast activity of adult hematopoietic stem cells

Steven M. Guthrie, Lisa M. Curtis, Robert N. Mames, Gregory G. Simon, Maria B. Grant, and Edward W. Scott

We have previously established a model inducing hematopoietic stem cell (HSC) production of circulating endothelial progenitor cells (EPCs) to revascularize ischemic injury in adult mouse retina. The unique vascular environment of the retina results in new blood vessel formation primarily from HSC-derived EPCs. Using mice deficient (−/−) in inducible nitric oxide synthase (iNOS) and endothelial nitric oxide synthase (eNOS), we show that vessel phenotype resulting from hemangioblast activity can be altered by modulation of the NO/NOS pathway. iNOS$^{-/-}$ or eNOS$^{-/-}$ animals were engrafted with wild-type (WT) HSCs expressing green fluorescence protein (*gfp*$^{+}$) and subjected to our adult retinal ischemia model. WT hemangioblast activity in adult iNOS$^{-/-}$ recipients resulted in the formation of highly branched blood vessels of donor origin, which were readily perfused indicating functionality. In contrast, eNOS$^{-/-}$ recipients produced relatively unbranched blood vessels with significant donor contribution that were difficult to perfuse, indicating poor functionality. Furthermore, eNOS$^{-/-}$ chimeras had extensive *gfp*$^{+}$ HSC contribution throughout their vasculature without additional injury. This neovascularization, via EPCs derived from the transplanted HSCs, reveals that the NO pathway can modulate EPC activity and plays a critical role in both blood vessel formation in response to injury and normal endothelial cell maintenance. (Blood. 2005;105:1916-1922)

Introduction

During embryogenesis, the hematopoietic and endothelial lineages arise from a common progenitor termed the hemangioblast.[1] We recently demonstrated that hemangioblast activity persists into adulthood by showing that adult hematopoietic stem cells (HSCs) produce both blood and blood vessels.[2] In adults, the relatively short lifespan of most blood cells necessitates replacement in large quantities each day to maintain homeostasis. Conversely, the endothelial vasculature in the eye can have up to a 4-year half-life in humans. When these vessels are replaced, it has been traditionally believed that the new endothelial cells (ECs) were derived solely from local EC proliferation. However, both ECs and endothelial progenitor cells (EPCs) were found in the circulation, posing the question whether cells of the vasculature can be formed from remote sources.[3,4] Multiple studies demonstrate the bone marrow (BM) origin of EPCs in a variety of ischemic and wound repair models.[5-8] In these models new vessel formation appears to be a combination of EC and EPC contributions, with ECs forming the majority of each new vessel. In contrast, ischemia or injury alone is not sufficient to induce neovascularization of the adult murine retina. Induction of retinal neovascularization requires both exogenous administration of vascular endothelial growth factor (VEGF) and ischemic injury. Providing both stimuli resulted in a highly proliferative retinopathy including new vessels protruding into the vitreous of the eye.[2] The pathology of our model is very similar to the proliferative stage of human diabetic retinopathy. Using this model, we demonstrated that the long-term self-renewing HSC was the clonal source of both blood and the newly formed retinal vasculature. Clonal hemangioblast activity was proven through long-term engraftment of a single HSC of a lethally irradiated recipient producing T-cell, B-cell, and macrophage blood lineages. The same cell also contributed significantly to the vascular endothelium of functional blood vessels. We and others have shown that fusion does not play a major role in this process.[9-11] Our basic results have since been confirmed in a variety of models.[10,12] The primary advantage of our retinal neovascularization model is predominance of the HSC-derived EPCs in forming new retinal vasculature, which can result in almost entirely donor EPC-derived vessels. In other injury models, much lower levels of EPCs have been found to contribute to new vessel formation making functional studies of the EPCs difficult (unpublished observation, 2002).[13]

In this study we examined the nitric oxide (NO) pathway to determine the effect of local NO synthase (NOS) activity on EPC-derived blood vessel formation. The presence of a NOS isoform specifically found in ECs (eNOS) hinted that NO influenced blood vessel formation and remodeling. NO also mediates

From the Program in Stem Cell Biology and Regenerative Medicine, University of Florida Shand's Cancer Center, Gainesville, FL.

Submitted September 9, 2004; accepted October 24, 2004. Prepublished online as *Blood* First Edition Paper, November 16, 2004; DOI 10.1182/blood-2004-09-3415.

Supported by National Institute of Health (NIH) grants HL70813, HL70738 (E.W.S.), and EY12601 (M.B.G.), and a grant from the Juvenile Diabetes Foundation (M.B.G. and E.W.S.). S.M.G. was supported by NIH Training Grant T32AR07603. E.W.S. is a Leukemia and Lymphoma Society Scholar.

E.W.S. has a financial interest in Regen Med, a company whose potential product was studied in the present work.

M.B.G. and E.W.S. contributed equally to the work.

The online version of the article contains a data supplement.

An Inside *Blood* analysis of this article appears in the front of this issue.

Reprints: Edward W. Scott, University of Florida, Academic Research Building R4-254, 1600 SW Archer Rd, Gainesville, FL 32610; e-mail: escott@ufl.edu; or Maria B. Grant, University of Florida, Academic Research Building R5-250, 1600 SW Archer Rd, Gainesville, FL 32610; e-mail: grantma@pharmacology.ufl.edu.

The publication costs of this article were defrayed in part by page charge payment. Therefore, and solely to indicate this fact, this article is hereby marked "advertisement" in accordance with 18 U.S.C. section 1734.

EC function and has been shown to influence blood vessel formation in several models of angiogenesis in vivo.[14,15] NO enhances neovascularization by acting as a downstream mediator of VEGF signaling.[16] In addition, increased local concentrations of NO stimulate proliferation and migration of ECs, both of which are essential for angiogenesis.[17-19] Consequently we hypothesized that the NO pathway would influence the process of neovascularization in the eye by directing the formation of EPC-derived vessels.

We found that the NO pathway is a significant regulator of neovascularization and can modulate hemangioblast activity by dictating the size and branching characteristics of blood vessels formed in response to ischemic or chronic injury. Our model provides a unique method of preferentially inducing EPC-driven repair of ischemic injury in the eye. The NO pathway also affects blood cell proliferation, migration, and mobilization.[13,16,17] The overlapping effects of the NO pathway in both blood and blood vessel formation further highlights the developmental relationship of the vascular and hematopoietic systems.

Materials and methods

Generation of eNOS and iNOS *gfp*$^+$ chimeric mice

All animal procedures were performed under approval of the University of Florida Animal Care and Use Committee and received IACUC approval. The C57BL/6, *gfp*$^+$ transgenic, eNOS, and inducible NOS (iNOS) knockout strains used were obtained from the Jackson Laboratory (Bar Harbor, ME). Genotyping of these animals was verified through polymerase chain reaction (PCR) analysis of tail biopsies to demonstrate the absence of the NOS genes (unpublished data, 2003). Radiation chimeras were produced by irradiating recipient animals (C57BL6 with 950 rads, NOS knockouts with 650 rads) followed by intravenous transplantation of up to 2500 sca-1, c-kit, lineage-negative (SKL) *gfp*$^+$ HSCs. The difference in radiation doses is due to the increased sensitivity of the knockout animals to radiation. It was found that 950 rads proved lethal to a high proportion of the treated knockout animals. For transplantation, HSCs were enriched from adult BM. Briefly, long bones in the legs were removed and the hollow marrow space flushed with Iscove modified Dulbecco medium (IMDM; Invitrogen, Carlsbad, CA) via a 26-gauge needle. Marrow was made into a single-cell suspension and plated onto treated plastic dishes in IMDM plus 20% fetal bovine serum (FBS; Summit Biotechnology, Fort Collins, CO) for 4 hours. Stromal and hematopoietic progenitor cells adhere; therefore nonadherent cells were collected and stained for sca-1, c-kit, and a lineage cocktail containing B220, CD11b, CD3, CD4, and Ter-119 (PharMingen, San Jose, CA).[2] *Gfp*$^+$ donor-derived engraftment was determined by fluorescence-activated cell sorting (FACS) analysis of peripheral blood from tail bleeds starting 1 month after transplantation and confirmed during each subsequent procedure. Animals that were not long-term engrafted were discarded from the study. During this time animals were given food and antibiotic (Bactrum; Pharmacal, Amityville, NY) water ad libitum, sustained under specific pathogen-free conditions, and kept on a 12-hour light/12-hour dark circadian cycle.

Induction of retinal neovascularization

Long-term durable hematopoietic reconstitution was confirmed by FACS analysis of peripheral blood 3 and 6 months after transplantation. Cohorts ($n = 10$) were identified with similar engraftment rates of peripheral blood mononuclear cells (all $> 70\%$ donor derived when normalized to donor *gfp*$^+$ animals) for subsequent experimentation. Matched cohorts were injected with saturating titers (1×10^9 PFU) of adeno-associated virus (AAV; VectorCore, University of Florida) expressing VEGF directly into the vitreous using a 36-gauge needle and Hamilton syringe. The dosage was determined by in vivo titering for maximal hemangioblast response. One month after viral infection the mice underwent laser treatment. An argon green laser system (HGM, Salt Lake City, UT) was used for retinal vessel photocoagulation with the aid of a 78-diopter lens as described.[2] The blue-green argon laser (wavelength 488-514 nm) is applied to various venous sites juxtaposed with the optic nerve. The venous occlusions are accomplished with more than 60 burns of 1-second duration, 50-mm spot size, and 50 to 100 mW intensity. Venous occlusion is readily visualized as a loss of downstream circulation resulting in a whitening of the vessel and cessation of circulating fluorescent dye administered before treatment into the bloodstream. The venous occlusion targets larger vessels in a semicircle arc around the retinal disk to establish ischemia in approximately one half of the retina.

Data collection and analysis

Mice were killed 4 weeks after laser treatment. Peripheral blood and BM were collected for analysis by flow cytometry with lineage-specific antibodies (CD11b, B220, CD4) conjugated to phycoerythrin (PE; BD Biosciences, San Jose, CA) to determine donor contribution. Then, 3 mL of 50 mg/mL tetramethyl rhodamine isothiocyanate-conjugated dextran (TRITC) 160 000 Da average molecular weight (Sigma, St Louis, MO) in phosphate-buffered paraformaldehyde (PFA; pH 7.4) was administered through the left ventricle to perfuse the vasculature. The perfusion was qualitated by gross observation of muscle contraction seen throughout the animal, a change in liver color as blood was replaced with the TRITC/PFA mix, and vasculature rupture in the nasal sinus. Experimental animals that did not demonstrate sufficient gross perfusion were not used for analysis because of the importance of vascular function measured via imaging in this model. Immediately after perfusion, eyes were removed and retinas dissected and whole mounted for confocal microscopy using Vectashield mounting medium (Vector Laboratories, Burlingame, CA) to inhibit photo-bleaching. The Olympus IX-70 microscope (Melville, NY), coupled to the Bio-Rad (Hercules, CA) Confocal 1024 ES system software, was used for confocal microscopy. To identify *gfp*$^+$ ECs in vasculature outside the retina, tissues and organs from the animals were dissected and frozen in Optimum Cutting Medium (OCT; Tissue-Tek, Torrance, CA) for cryosectioning and immunocytochemistry. Sections were cryosectioned at a thickness of 10 μm, flat mounted with Vectashield, and analyzed by fluorescent microscopy to detect *gfp*$^+$ cells. Adjacent sections were stained with an endothelial-specific surface marker MECA-32 (PharMingen) followed by secondary staining with goat anti–rat IgG conjugated to Texas red (PharMingen). Rat IgG isotype in the place of the primary served as the "no stain" control. All immunostained sections were mounted with Vectashield containing DAPI (4,6 diamidino-2-phenylindole).

Detection and localization of NOS produced in NOS-deficient animals

To compare the amount of NO produced by the various isoform knockouts, iNOS- and eNOS-specific antibodies (PharMingen) were used to test levels seen under normal conditions and in situations when a specific isoform is missing. C57BL/6, iNOS$^{-/-}$, and eNOS$^{-/-}$ animals were quantitated for NOS expression in parallel. Animals were humanely killed and the eyes enucleated as described except these animals were not perfused with the TRITC/PFA mixture. The dissected retinas were then stained with iNOS-specific (Abcam, Cambridge, MA) and eNOS-specific (PharMingen) primary antibodies used to detect iNOS and eNOS protein levels within dissected retinas. Goat antirabbit conjugated to fluorescein isothiocyanate (FITC; Sigma, St Louis) was used as the secondary antibody. To facilitate the visualization of colocalization of the NOS protein in the vessel endothelial cells, retinas were stained with peanut agglutinin conjugated to phycoerythrin (PE).

Results

iNOS and eNOS *gfp*$^+$ chimeras demonstrated robust HSC engraftment

To directly assess the role of NOS activity in the promotion of HSC transdifferentiation into blood vessels, we inserted transplants in

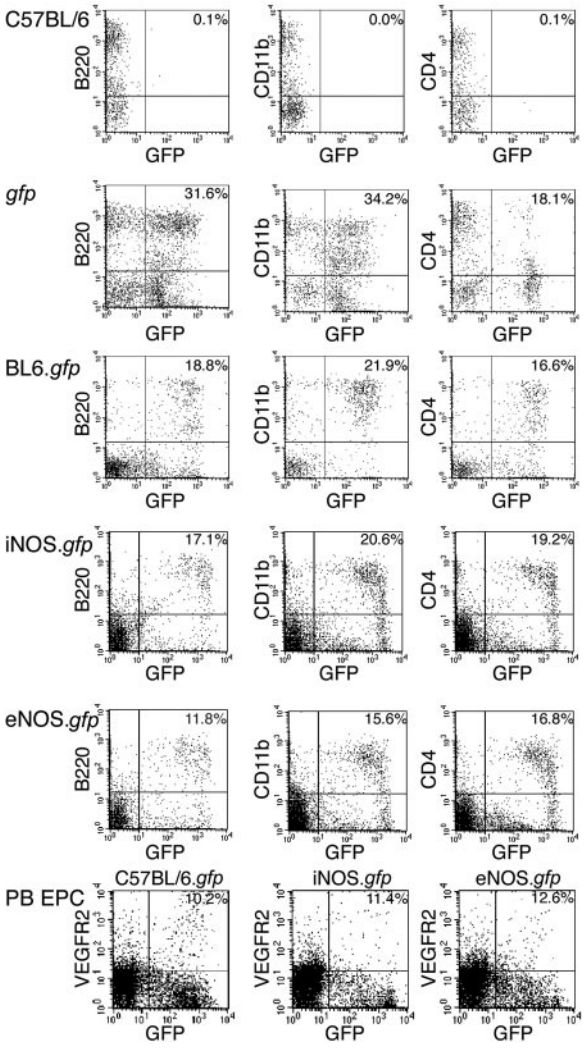

Figure 1. Long-term, multilineage, donor *gfp* peripheral blood engraftment. Peripheral blood mononuclear cells were analyzed by flow cytometry 3 months after transplantation. The first column is B cells expressing B220, the second column is macrophages expressing CD11b, and the third column is T cells expressing CD4. The top row is a C57BL/6 and the second row is a *gfp* donor strain for reference controls. The third row is a representative C57BL/6.*gfp* chimeric mouse. The fourth row is a representative iNOS.*gfp,* and the fifth row is a eNOS.*gfp.* The bottom row shows peripheral blood with circulating VEGFR2$^+$ cells in C57BL/6.*gfp,* iNOS.*gfp,* and eNOS.*gfp* animals. Numbers in the top right corner are percentages of doubly lineage-stained and *gfp*$^+$ cells. PB indicates peripheral blood.

cohorts of C57BL6, iNOS$^{-/-}$, and eNOS$^{-/-}$ animals with highly enriched *gfp*$^+$ HSCs to produce radiation chimeras designated C57BL6.*gfp*, iNOS.*gfp*, and eNOS.*gfp*, respectively. The eNOS$^{-/-}$ animals are not healthy and exhibit reduced litter sizes, growth, and limb abnormalities.[20] This sickliness is exacerbated with BM ablation such as irradiation as shown by diminished HSC proliferation.[13] Consequently, eNOS cohorts received a minimum of 2500 highly enriched HSCs to ensure robust donor engraftment due to the reduced radiation level tolerated by the knockout animals. All cohorts compared were age matched and exhibited matched percentages of donor engraftment levels prior to ischemic model, and recipients that were robustly reconstituted by donor HSCs ($> 70\%$ donor-derived myeloid cells as the benchmark) subsequently underwent our model of ischemic injury to induce adult retinal neovascularization ($n > 10$ for all cohorts). Peripheral blood from a typical BL6 (Figure 1 top row) and *gfp*$^+$ (Figure 1 second row) mouse are shown as a reference for comparison of the engraftment levels of the test animals. The enriched HSC populations used for transplantation into the NOS-deficient mice were isolated using the same protocol previously used for single-cell transplants in BL6 animals (Figure 1 third row).[2] Multilineage hematopoietic engraftment was confirmed more than 3 months after transplantation by flow cytometry analysis of peripheral blood prior to model induction and confirmed at the time of tissue harvest more than 6 months after transplantation for all cohorts (Figure 1 fourth row, iNOS$^{-/-}$ and fifth row, eNOS$^{-/-}$). To demonstrate that HSC-derived EPCs are present in the circulation and available for contribution to neovascularization, peripheral blood was drawn and analyzed for donor EPCs. Both irradiated and treated animals and untreated animals had significant amounts ($> 10\%$) of circulating EPCs contained in the nucleated blood cells (Figure 1 bottom row). We found slightly increased levels of circulating *gfp*$^+$ EPCs in the experimental animals, which could hint that irradiation, VEGF, and ischemic injury are signaling for increased BM EPC production (unpublished observation). This phenomenon will be examined further.

The NOS pathway affects blood vessel formation

After induction of retinal ischemia by laser ablation injury, C57BL6.*gfp* chimeras produced a variety of *gfp*$^+$ blood vessels at the sites of injury ranging from small capillaries to larger vessels. In C57BL6.*gfp* chimeras, size was most likely dictated by the degree of the laser injury (Figure 2C,E,G), and no *gfp*$^+$ contribution to vasculature was observed in control eyes (Figure 2D,F). iNOS.*gfp* chimeras produced primarily small, highly branched blood vessels that perfused readily in treated eyes (Figure 3E,G). These animals had limited donor EPC contribution in contralateral untreated eyes (Figure 3D,F). Strikingly, eNOS.*gfp* chimeras only

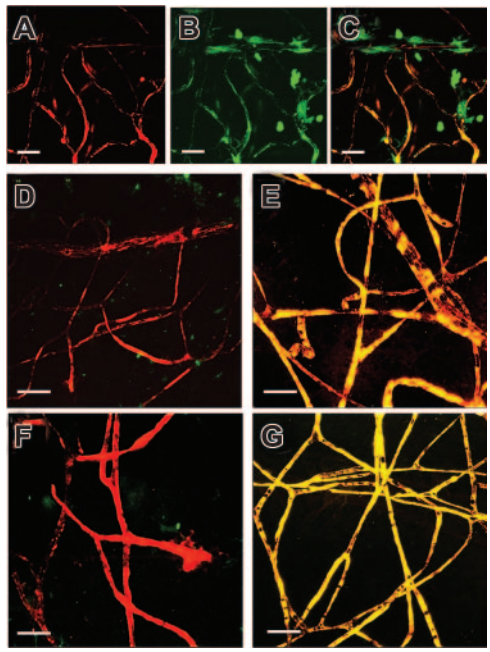

Figure 2. WT retinal neovascularization. C57BL/6.*gfp* chimeric mice underwent the retinal ischemia model followed by perfusion with TRITC before eye enucleation and confocal imaging of the retinas. Panel A is the red channel alone. Panel B is the green channel alone. Panel C is the merged image of the red and green channels. Yellow areas are colocalization of donor-derived *gfp* cells and TRITC-perfused patent vessels. Note: All further panels in each figure are from red and green channel merged images unless noted. Panels D and F are contralateral untreated control eyes and E and G are experimental eyes from the same respective mice. Original magnification × 60; size bar about 10 μm.

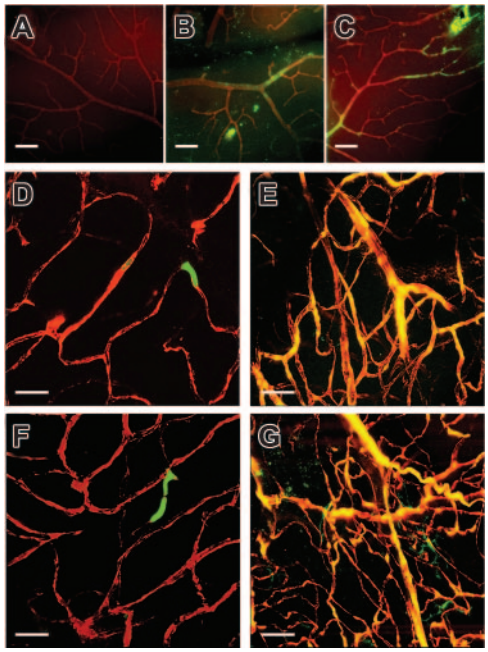

Figure 3. iNOS expression in the retina and iNOS modulation of retinal neovascularization. iNOS$^{-/-}$ retinas were stained with NOS isoform-specific antibodies. In panels A-C, red depicts agglutinin staining for vessel visualization and green represents NOS antibody positive regions. Panel A is an iNOS$^{-/-}$ retina stained with the iNOS-specific antibody. Panels B and C are iNOS$^{-/-}$ stained with eNOS isoform-specific antibody. The iNOS.*gfp* chimeric mice underwent the retinal ischemia model followed by perfusion with TRITC before eye enucleation and confocal imaging of the retinas. Panels D through G are red and green channel merged images from control (D,F) and treated (E,G) retinas. Original magnification × 60; size bar about 10 μm.

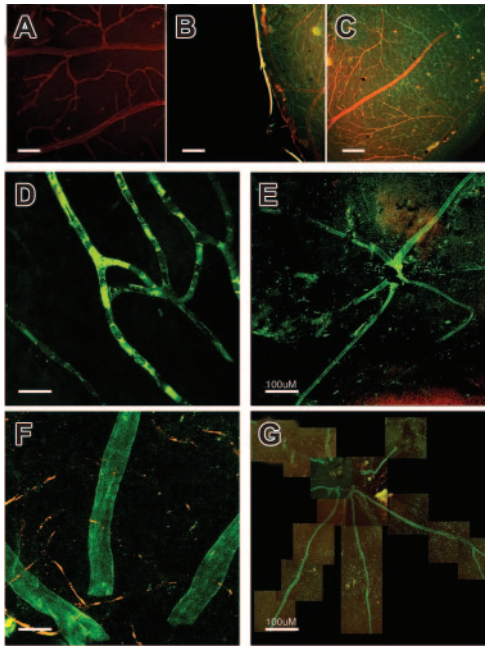

Figure 4. eNOS expression in the retina and eNOS modulation of retinal neovascularization. eNOS$^{-/-}$ retinas were stained with NOS isoform-specific antibodies. In panels A-C, red depicts agglutinin staining for vessel visualization and green represents NOS antibody positive regions. Panel A is an eNOS$^{-/-}$ retina stained with the eNOS-specific antibody. Panels B and C are eNOS$^{-/-}$ stained with iNOS isoform-specific antibody. eNOS.*gfp* chimeric mice underwent the retinal ischemia model followed by perfusion with TRITC before eye enucleation and confocal imaging of the retinas. Panels D-G are red and green channel merged images from control (D,F) and treated (E,G) retinas. Original magnifications × 60 (D), × 4 (E), and × 10 (F). Panel G is a composite of images at original magnification × 60. Size bar is about 10 μM unless noted as about 100 μm.

produced relatively large and unbranched vessels regardless of ischemic insult (Figure 4D-G). These vessels tended to perfuse poorly despite their large size, which is consistent with the known vascular defects of eNOS$^{-/-}$ animals. Of note, this phenotype was not due to the inability to visualize the red dye in large vessels due to the fact that the fluorescent perfusant can be easily visualized in B6 control vessels of similar size. To further demonstrate that new vessels originate from functional vasculature, we have provided a supplemental video on the *Blood* website; see the Supplemental Video link at the top of the online article. In the video each 1 μm section of a confocal Z-series is shown in order. A perfused and functional vessel can be seen deep within the retina tissue. Sprouting out and up into the vitreous space is a nonperfused vessel that is completely donor-derived. Whether this lack of vessel functionality is due to some vascular blockage or some alternative defect is not known. In addition, the branching characteristics of the 3 strains were markedly different suggesting that the NO pathway functions in vessel organization. Total branch points of *gfp* vessels per × 60 field of view were counted for each genotype (Figure 5). C57BL6 model control cohorts averaged about 18 branch points per visual field. The iNOS$^{-/-}$ recipients had nearly 3-fold more branch points per field, whereas eNOS$^{-/-}$ recipients averaged less than one branch point per field.

eNOS deficiency promotes HSC-derived EPC contribution to vasculature

To further examine the role of NOS in neovascularization, we examined retinas from the nontreated contralateral control eyes vis-à-vis the injured retinas of WT, iNOS$^{-/-}$, and eNOS$^{-/-}$ recipients. This was done to elucidate whether NOS could drive the HSC contribution to the vasculature without ischemic injury and growth factor administration. iNOS$^{-/-}$ animals responded in a similar fashion to WT animals with production of *gfp*$^{+}$ HSC-derived vessels only in the VEGF-treated and injured retina (Figure 3E,G), but substantially reduced contribution was found in the retinas from the contralateral untreated eye (Figure 3D,F). Unexpectedly, retinas from eNOS$^{-/-}$ recipients, which as described in other studies have systemic vascular dysfunction,[21] demonstrated robust *gfp*$^{+}$ HSC-derived contribution to the preexisting vascular endothelium of both test (Figure 4E,G) and control eyes (Figure 4D,F). The profound contribution of HSC-derived *gfp*$^{+}$ cells to the

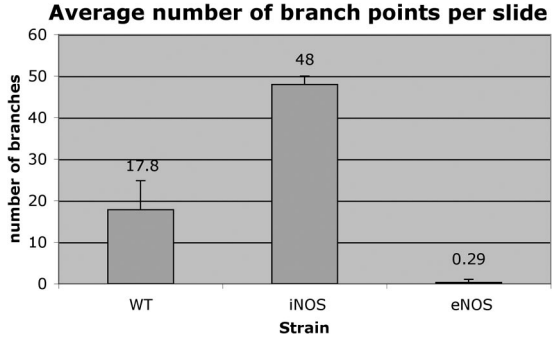

Figure 5. Branching characteristics. Confocal Z-series images were compressed and counted "blindly" for number of vessel branch points per image. C57BL/6.*gfp* retinas averaged 17.8 branches per image (n=5). iNOS.*gfp* retinas averaged 48 branch points per image (n=4). eNOS.*gfp* retinas averaged 0.29 branch points per image (n=38). The blood vessels of iNOS$^{-/-}$ retinas were 2.7 times more branched than WT animals ($P < .0001$), whereas eNOS$^{-/-}$ retinas were 61.5 times less branched than WT ($P < .0002$). Error bars indicate standard errors of the means.

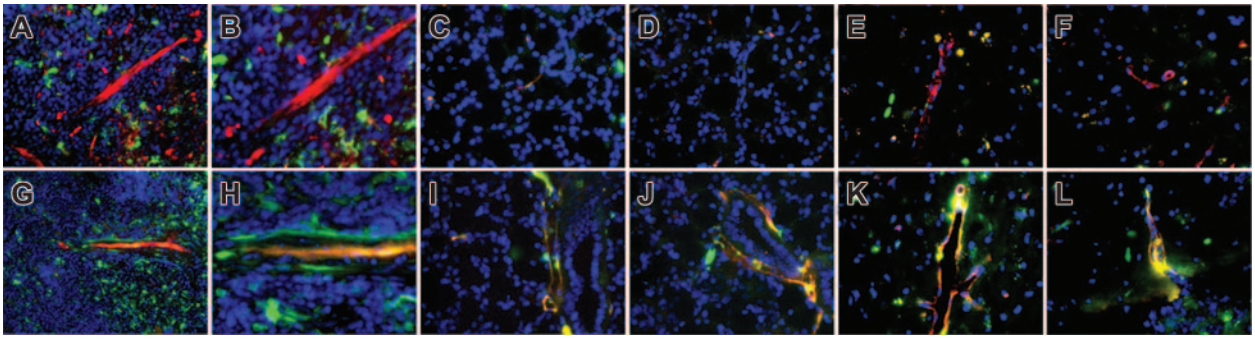

Figure 6. Chronic vascular injury in eNOS. *gfp* chimeras induces widespread hemangioblast activity from adult HSCs. Spleen (A-B,G-H), thymus (C-D,I-J), and brain (E-F,K-L) were harvested from TRITC-perfused animals and 10-μm cryosections were prepared and mounted with Vectashield plus DAPI. iNOS.*gfp* (A-F) and eNOS.*gfp* (G-L) chimeras were examined by fluorescence microscopy. Donor *gfp* HSC-derived cells are green and the TRITC perfusant is red. Original magnification × 40 for panels A and G. All remaining panels are original magnification × 64.

untreated retinas of eNOS$^{-/-}$ recipients strongly suggested that lack of eNOS causes chronic vascular injury and is sufficient to induce hemangioblast activity from the HSCs.

eNOS$^{-/-}$ recipients have whole body vascular remodeling by WT HSCs/EPCs

To prove eNOS$^{-/-}$ is a chronic disease state where HSCs contribute to the vasculature, we examined vessels throughout the entire eNOS$^{-/-}$ mouse. To determine the extent of donor *gfp*$^+$ HSC contribution to the overall vascular system we harvested multiple tissues (spleen, thymus, brain, kidney, liver, muscle, skin, and gut) from the C57BL6.*gfp*, iNOS.*gfp*, and eNOS.*gfp* chimeras (n = 10/cohort). Each of these animals had demonstrated long-term, multilineage hematopoietic engraftment and had undergone the retinal ischemia model. At 1 month after the induction of retinal ischemia the animals were humanely killed and perfused, and harvested tissues were sectioned. Samples were examined by fluorescent microscopy for *gfp*$^+$ contributions to the vasculature. Results for the spleen, thymus, and brain are shown (Figure 6). In all cases the C57BL6.*gfp* and iNOS.*gfp* yielded similar results: few *gfp*$^+$ cells being incorporated into blood vessels in any tissue outside of the treated retina (Figure 6A-F and data not shown). This indicates that in our model whole body irradiation alone and the lack of the iNOS isoform is not sufficient for induction of HSC contribution to vasculature in tissues that are not treated further. In contrast, eNOS.*gfp* chimeras exhibited robust *gfp*$^+$ contributions to the vasculature (colocalization of *gfp*$^+$ with perfused TRITC) in all tissues examined (Figure 6G-L and data not shown). The absence of eNOS creates a pathologic vascular condition where HSCs are induced to contribute to vascular repair throughout an organism.

Donor-derived vascular ECs are phenotypically distinct from donor HSCs

To ascertain the endothelial cell nature of the *gfp*$^+$ cells surrounding the vessel lumens, tissue sections were stained for the pan-endothelial cell marker MECA-32. ECs were then scored for the presence of both MECA-32$^+$ and *gfp*$^+$ cells via fluorescent microscopy. Splenic sections demonstrate the characteristic results observed in all tissues studied (Figure 7). Donor-derived hematopoietic cells in the spleen serve as internal negative staining controls for MECA-32 in each section. WT animals showed occasional *gfp*$^+$, MECA-32$^+$ ECs in the brain (closest organ to the site of VEGF administration) with the majority of tissues such as the spleen (Figure 7A-D), kidney, liver, and muscle showing no donor-derived ECs. This shows that our model recapitulates what we and others have observed that under normal physiologic conditions there is little HSC contribution to ECs. iNOS$^{-/-}$ animals, which exhibit minor systemic vascular defects, had occasional *gfp*$^+$, MECA-32$^+$ ECs in the spleen (Figure 7E-H) and other tissues. Overall *gfp*$^+$ HSC-derived contribution to the vasculature of iNOS$^{-/-}$ animals, outside the area of retinal ischemia, was at most 1% in more than 150 tissue sections examined for MECA-32$^+$ vessels. Robust *gfp*$^+$ donor-derived EC production was observed in eNOS$^{-/-}$ recipients. Most vessels (> 50%) were remarkably large, and most showed extensive *gfp*$^+$ HSC-derived MECA-32$^+$ EC contributions as seen in the spleen (Figure 7I-P) and other tissues examined. The *gfp*$^+$ MECA-32$^+$ cells seen outside the intima of the vessels are most likely due to extensive remodeling occurring to relieve the ischemia and alleviate chronic injury. The pathology of this phenotype will be examined.

Detection and localization of NOS produced in knockout animals

Because NOS knockout animals still have functional NOS genes, the pathology observed may be due to a dysregulation or compensatory NO production by the remaining isoforms. To ascertain the influence and determine the expression of NOS in animals lacking

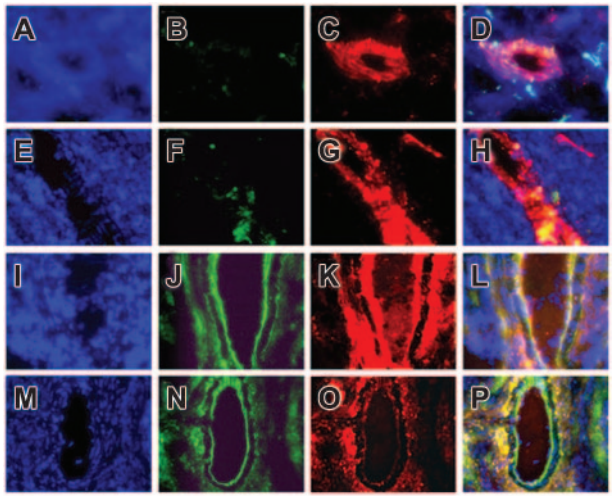

Figure 7. MECA-32$^+$, *gfp*$^+$, HSC-derived endothelial cells in eNOS.*gfp* spleens. Splenic cryosections were prepared from C57BL/6.*gfp* (A-D), iNOS.*gfp* (E-H), and eNOS.*gfp* (I-P) chimeras. Sections were stained with anti-MECA-32 antibody and a Texas red-conjugated secondary antibody to delineate vascular endothelium. Sections were mounted with DAPI (A,E,I,M) to delineate nuclei with blue fluorescence, examined for *gfp* expression (B,F,J,N) via green fluorescence, or MECA-32 staining (C,G,K,O) via red fluorescence. (D,H,L,P) Merged images of the DAPI, *gfp*, and MECA-32 Texas red stains. Original magnifications × 64 (A-L) and × 32 (M-P).

one specific NOS isoform, retinas were dissected and stained with NOS isoform-specific antibodies from mice that had not undergone HSC transplantation or the neovascularization model. iNOS$^{-/-}$ (Figure 3A-C) and eNOS$^{-/-}$ (Figure 4A-C) animals were compared for NOS expression in parallel. Animals were killed and the eyes enucleated. Following staining with NOS isoform-specific antibodies and peanut agglutinin, retinas were then imaged through fluorescence microscopy. Figures 3A and 4A each demonstrate that in each knockout strain the isoform that is deleted is not expressed in vivo at detectable levels. iNOS$^{-/-}$ animals have normal amounts of eNOS expressed; however, eNOS$^{-/-}$ retinas demonstrate an increase in iNOS expression as seen throughout both the large, and particularly, the smaller vessels. This demonstrates that there is compensatory up-regulation of iNOS expression in eNOS knockout retinas indicating a dysregulation in amount of NO produced. This dysregulation may account for the pathologic blood vessel formation observed in these animals.

Discussion

Although few topics have stirred more debate recently, the promise of HSC plasticity still holds tremendous potential as cell therapy for many debilitating diseases. HSCs have been shown to transdifferentiate into a variety of nonhematopoietic tissues in various organs such as the vasculature, liver, brain, cardiac muscle, intestine, and pancreas.[2,22-26] Nevertheless, attempts to recapitulate these studies have found limited HSC plasticity.[27,28] Major questions have been raised concerning HSC fusion[11]; however, the lack of fusion seen in diverse tissues is remarkable and does not appear to be the predominant method of HSC production of ECs.[10] Importantly, circulating donor-derived EPCs retain normal 2N ploidy in our model.[9]

Circulating EPCs were initially described in the late part of the last century.[4] We used a novel model of retinal neovascularization in combination with single HSC transplantation to demonstrate that EPCs are derived from HSCs and represent an alternative developmental fate.[2] The low turnover rate of normal vascular endothelium results in infrequent EC replacement in the absence of injury. The unique physiology of adult retinal vasculature results in new vessels being primarily formed from circulating EPCs rather than resident EC proliferation. Therefore, the model was ideally suited for determining the cell of EPC origin to the BM.

In this study we begin the exploration of what dictates EC- versus EPC-driven vascular repair. Clearly in normal ischemia, as observed in the hindlimb model, ECs contribute primarily to reperfusion.[13,14] However, in our retina ischemia model we find donor-derived EPCs contribute to the majority of neovascularization. These conflicting observations were resolved through further study of eNOS$^{-/-}$ mice. In these animals the retina vasculature, along with the vasculature of other unrelated organs, was replaced with donor-derived EPCs independent of growth factor administration. We conclude that resident eNOS$^{-/-}$ ECs are in a state of chronic injury resulting in a competitive disadvantage with respect to WT donor-derived EPCs. This resulted in widespread WT donor-derived EPC contribution to the vasculature throughout the eNOS$^{-/-}$ recipients. This finding suggests that the NO pathway may be a critical in determining whether ECs or EPCs contribute to neovascularization. It is very interesting to note that eNOS has recently been implicated in hematopoietic progenitor mobilization from the BM.[13]

NOS activity also dictates the general size and branch characteristics of new blood vessels formed in response to ischemic injury. Donor WT HSCs transplanted into iNOS$^{-/-}$ recipients (retaining eNOS activity) produce highly branched vessels that are generally smaller in size. These vessels are functional as measured by perfusion of marker dye. In contrast, eNOS$^{-/-}$ recipients produced primarily unbranched vessels of large size in response to injury. This response was in addition to the widespread vascular remodeling by donor HSCs seen throughout the eNOS$^{-/-}$ recipients. These vessels were also difficult to perfuse indicative of the general vascular dysfunction described in these knockouts.[21] Note that in Figure 4E,G low-magnification images allow visualization of large portions of retina. The abrupt end of vessels in the center occurs where the retinal optic disc was separated from the incoming optic nerve/vessel bundle. The ability to dictate the general size and type of vessel formed by HSCs/progeny in response to ischemic injury by altering NOS activity may allow specific remodeling of vascular beds with targeted treatment regimes. Several commonly used pharmaceuticals available affect either specific NOS isoform activity or NO levels. We are currently testing their effects on hemangioblast activity in our model. They may allow for the dissection of the EC to EPC mechanism described or could potentially provide therapy for vascular defects by dictating vessel branching and functionality.

The role of HSCs in production of EPCs is not surprising with recent groups demonstrating that an NO defect decreases BM mobilization.[13,16] Conversely, overexpression of eNOS generates an increase in vessel formation in response to ischemia.[29] We now show that donor WT HSCs transplanted into iNOS$^{-/-}$ recipients are functioning in an environment where local NO production is similar to what is seen in WT, non-VEGF–induced conditions due to the eNOS isoform, which is expressed normally. Contrastingly, eNOS$^{-/-}$ recipients produced primarily unbranched, nonfunctioning vessels of large size observed throughout the vasculature of the entire body. Without the basal levels of NO produced by eNOS, we found that there is a compensatory up-regulation of iNOS causing greater NO production. This triggers pathologic vessel turnover and drives EPC production of blood vessels. We must note that standard methods of direct or indirect NO detection are primarily limited to in vitro studies and we were unsuccessful in our attempts to adapt the methodology for in vivo conditions such as a whole mounted retina. As a result, the detection of NO levels is not directly measured and our data represent measurements of NOS isoforms present and not the amount of NO produced. Clearly, lacking one NOS isoform activity has significant consequences for EPC-driven neovascularization. Furthermore, although VEGF has been shown to be an upstream mediator of NO,[30] these 2 pathways can function independently in neovascularization because modification of the NO pathway independent of VEGF treatment affects blood vessel formation as seen in eNOS$^{-/-}$ animals. The regulation of NOS activity as a means to influence the remodeling of vascular beds may provide specific treatment regimes, and this model is an excellent system for work investigating the NO pathway on hemangioblast activity. With this understanding of the NO pathway, administration of agents that will modulate hemangioblast function may make an attractive therapy for pathologic vascular diseases.

Acknowledgments

We thank Tim Vaught for confocal imaging and all members of the Scott and Grant laboratories for additional technical support.

References

1. Nishikawa SI, Nishikawa S, Kawamoto H, et al. In vitro generation of lymphohematopoietic cells from endothelial cells purified from murine embryos. Immunity. 1998;8:761-769.
2. Grant MB, May WS, Caballero S, et al. Adult hematopoietic stem cells provide functional hemangioblast activity during retinal neovascularization. Nat Med. 2002;8:607-612.
3. George F, Poncelet P, Laurent JC, et al. Cytofluorometric detection of human endothelial cells in whole blood using S-Endo 1 monoclonal antibody. J Immunol Methods. 1991;139:65-75.
4. Asahara T, Takahashi T, Masuda H, et al. VEGF contributes to postnatal neovascularization by mobilizing bone marrow-derived endothelial progenitor cells. EMBO J. 1999;18:3964-3972.
5. Asahara T, Masuda H, Takahashi T, et al. Bone marrow origin of endothelial progenitor cells responsible for postnatal vasculogenesis in physiological and pathological neovascularization. Circ Res. 1999;85:221-228.
6. Crosby JR, Kaminski WE, Schatteman G, et al. Endothelial cells of hematopoietic origin make a significant contribution to adult blood vessel formation. Circ Res. 2000;87:728-730.
7. Takahashi T, Kalka C, Masuda H, et al. Ischemia- and cytokine-induced mobilization of bone marrow-derived endothelial progenitor cells for neovascularization. Nat Med. 1999;5:434-438.
8. Shi Q, Rafii S, Wu MH, et al. Evidence for circulating bone marrow-derived endothelial cells. Blood. 1998;92:362-367.
9. Cogle CR, Wainman DA, Jorgensen ML, Guthrie SM, Mames RN, Scott EW. Adult human hematopoietic cells provide functional hemangioblast activity. Blood. 2004;103:133-135.
10. Bailey AS, Jiang S, Afentoulis M, et al. Transplanted adult hematopoietic stem cells differentiate into functional endothelial cells. Blood. 2004; 103:13-19.
11. Alvarez-Dolado M, Pardal R, Garcia-Verdugo JM, et al. Fusion of bone-marrow-derived cells with Purkinje neurons, cardiomyocytes and hepatocytes. Nature. 2003;425:968-973.
12. Otani A, Kinder K, Ewalt K, Otero FJ, Schimmel P, Friedlander M. Bone marrow-derived stem cells target retinal astrocytes and can promote or inhibit retinal angiogenesis. Nat Med. 2002;8:1004-1010.
13. Aicher A, Heeschen C, Mildner-Rihm C, et al. Essential role of endothelial nitric oxide synthase for mobilization of stem and progenitor cells. Nat Med. 2003;9:1370-1376.
14. Murohara T, Asahara T, Silver M, et al. Nitric oxide synthase modulates angiogenesis in response to tissue ischemia. J Clin Invest. 1998; 101:2567-2578.
15. Ando A, Yang A, Mori K, et al. Nitric oxide is proangiogenic in the retina and choroid. J Cell Physiol. 2002;191:116-124.
16. Fukumura D, Gohongi T, Kadambi A, et al. Predominant role of endothelial nitric oxide synthase in vascular endothelial growth factor-induced angiogenesis and vascular permeability. Proc Natl Acad Sci U S A. 2001;98:2604-2609.
17. Ziche M, Morbidelli L, Masini E, et al. Nitric oxide mediates angiogenesis in vivo and endothelial cell growth and migration in vitro promoted by substance P. J Clin Invest. 1994;94:2036-2044.
18. Morbidelli L, Chang CH, Douglas JG, Granger HJ, Ledda F, Ziche M. Nitric oxide mediates mitogenic effect of VEGF on coronary venular endothelium. Am J Physiol. 1996;270:H411-415.
19. Noiri E, Lee E, Testa J, et al. Podokinesis in endothelial cell migration: role of nitric oxide. Am J Physiol. 1998;274:C236-244.
20. Gregg AR, Schauer A, Shi O, Liu Z, Lee CG, O'Brien WE. Limb reduction defects in endothelial nitric oxide synthase-deficient mice. Am J Physiol. 1998;275:H2319-2324.
21. Yang XP, Liu YH, Shesely EG, Bulagannawar M, Liu F, Carretero OA. Endothelial nitric oxide gene knockout mice: cardiac phenotypes and the effect of angiotensin-converting enzyme inhibitor on myocardial ischemia/reperfusion injury. Hypertension. 1999;34:24-30.
22. Petersen BE, Bowen WC, Patrene KD, et al. Bone marrow as a potential source of hepatic oval cells. Science. 1999;284:1168-1170.
23. Lagasse E, Connors H, Al-Dhalimy M, et al. Purified hematopoietic stem cells can differentiate into hepatocytes in vivo. Nat Med. 2000;6:1229-1234.
24. Brazelton TR, Rossi FM, Keshet GI, Blau HM. From marrow to brain: expression of neuronal phenotypes in adult mice. Science. 2000;290: 1775-1779.
25. Orlic D, Kajstura J, Chimenti S, et al. Bone marrow cells regenerate infarcted myocardium. Nature. 2001;410:701-705.
26. Krause DS, Theise ND, Collector MI, et al. Multi-organ, multi-lineage engraftment by a single bone marrow-derived stem cell. Cell. 2001;105:369-377.
27. Castro RF, Jackson KA, Goodell MA, Robertson CS, Liu H, Shine HD. Failure of bone marrow cells to transdifferentiate into neural cells in vivo. Science. 2002;297:1299.
28. Wagers AJ, Sherwood RI, Christensen JL, Weissman IL. Little evidence for developmental plasticity of adult hematopoietic stem cells. Science. 2002;297:2256-2259.
29. Amano K, Matsubara H, Iba O, et al. Enhancement of ischemia-induced angiogenesis by eNOS overexpression. Hypertension. 2003;41:156-162.
30. Risau W. Mechanisms of angiogenesis. Nature. 1997;386:671-674.